*J. Fluid Mech.* (1978), *vol.* 84, *part* 4, *pp.* 717–741
*Printed in Great Britain*



# The wave system attached to a finite slender body in a supersonic relaxing gas stream

By Y. L. SINAI† AND J. F. CLARKE

Department of Aerodynamics, Cranfield Institute of Technology, Bedford MK43 0AL, England

(Received 9 May 1977)

The results of a companion paper are extended to encompass the flow about smooth, but otherwise general body shapes. The wave behaviour depends on three important parameters, namely the body thickness ratio $\epsilon$, the quantity $\delta$, which is proportional to the difference between the frozen and equilibrium sound speeds, and the ratio $\lambda$ of a relaxation time to a characteristic flow time. Both analytical and numerical solutions have been obtained; account is taken of nonlinearity for complete spectra of the three parameters, enabling an assessment to be made of the evolution of the wave forms for a host of situations. In particular, it is possible to predict the structures of the shock waves in various regions, and it transpires that under certain conditions vibrational relaxation can overwhelm other dissipative effects.

## 1. Introduction

An aircraft moving supersonically produces a complicated shock pattern, and far from the aircraft these waves become dominated by the head and tail shocks. A theory based solely on transport phenomena indicates that the fine-structures of the shocks correspond to the classical, Taylor, one-dimensional profile (Lighthill 1956, p. 287) superimposed on the discontinuous field, and the thicknesses of the shocks normally remain small except at very large distances (Chong & Sirovich 1973). However, field measurements have divulged shock thicknesses much greater than those expected on this basis (Lilley 1965; Pierce & Maglieri 1972), and the present study aims to clarify this problem by formally solving the axisymmetric configuration.

It is well known that non-equilibrium phenomena can have significant effects on the propagation of waves through a gas (see, for example, Clarke & McChesney 1976). The probable relevance of relaxation effects to the sonic boom (Hodgson & Johannesen 1971; Hodgson 1973) constitutes one reason for re-opening the question of wave propagation through a relaxing gas; the present theory encompasses both chemical and thermal non-equilibrium, but this paper is aimed primarily at wave propagation through atmospheric air, where the vibrational relaxation of diatomic molecules is the pertinent process. A variety of configurations, both linear and nonlinear, have been studied analytically in the past (e.g. Lighthill 1956; Lick 1967; Clarke & McChesney 1976; representative Russian work may be found in the papers by Kraiko 1966; Ryzhov 1971; Rudenko, Soluyan & Khokhlov 1974; Tkalenko 1975); although some early work exists on the linear theory of axially symmetric flow, with one exception

† Present address: Department of Applied Mathematical Studies, University of Leeds, England.

(Clarke & Sinai 1977) there has been no attempt to date to analyse the nonlinear fi field of such a flow. Numerical and semi-empirical techniques (e.g. Stephenson 196( Sedney & Gerber 1963) are of course useful, particularly when disturbances are larg but closed-form solutions, if attainable, are more desirable. In a companion pape Clarke & Sinai (1977, hereafter referred to as I) presented results for the general linea theory in regions where its predictions begin to break down, and went ahead to analys the nonlinear waves attached to a cone. The purpose of the present paper is to exten the analysis to general (but smooth) body shapes.

An interesting study of the problem has been carried out by Chou & Chu (1971; se also Chou 1972), but their technique is based on the method of characteristic para meters, and it consequently cannot be used to examine the truly distant flow fielc (Clarke 1965).

The basic small parameter in the present theory is $\epsilon$, the thickness ratio of the body, and all other small (or large) parameters are measured against it. In fact, we shall use the second-order frozen theory (Landahl & Lofgren 1973) as a basis for comparison whenever we have to decide whether a given term is negligible or not.

A convenient measure of the energy content of the non-equilibrium mode is the quantity $\delta \propto a_{f0}^2/a_{e0}^2 - 1$, where $a_{f0}$ and $a_{e0}$ are the free-stream frozen and equilibrium sound speeds respectively; when the process under consideration is internal energy relaxation, $\delta$ is related to the fraction of the total thermal energy which is contributed by the relaxing mode. An important feature of the vibrational relaxation of atmospheric oxygen and nitrogen is the smallness of $\delta$ (e.g. Hodgson & Johannesen 1971). With $\delta$ typically lying between $10^{-4}$ and $10^{-3}$, this process has understandably been neglected during calculations of the flow field near the body. However, as was pointed out by Hodgson & Johannesen (1971), geometric attenuation can give rise to disturbances as small as $\delta$ (Whitham 1952), and when considering the far field, one cannot dismiss relaxation as a higher-order effect.

Of the studies published in the West, the pioneering work on the small-$\delta$ situation is due to Blythe (1969) and Ockendon & Spence (1969). Both papers deal with the piston problem, although Blythe includes the steady, two-dimensional, supersonic flow in the small-$\delta$ context. Both studies have been confined (explicitly or implicitly) to $\delta = O(1)$ and $\delta = O(\epsilon)$, and it transpires (Sinai 1975; Clarke & Sinai 1977) that the comparable small-$\delta$ situation in the axisymmetric problem is $\delta = O(\epsilon^4)$; in contrast to previous studies, Clarke & Sinai (1977) analysed the complete spectrum of $\delta$ between unity and its 'small' value.

In passing we note that in typical aeronautical situations $\delta$ lies a little above the very small value of $\epsilon^4$; for example, if $\epsilon = 0{\cdot}05$, $\epsilon^4 \simeq 10^{-5}$, which is an order of magnitude less than $\delta$ at sea level (it should however be emphasized that $\delta$ *decreases with altitude*).

A third important parameter is the ratio of the relaxation time $\tau'$ to a characteristic flow time. It so happens that $\tau'$ is very sensitive to the humidity (e.g. Sutherland 1975), and typically it varies between $10^{-3}$ s and $10^{-6}$ s under dry and humid conditions respectively (the reader is referred to the pertinent comments by Hodgson & Johannesen 1971).

Seeing that some of the present analysis closely follows that in I, we shall avoid superfluous repetitions and the reader is referred to I for preliminary details. Section 4 deals with ord $\delta > \epsilon^4$, including the near-frozen front and the near-equilibrium fully dispersed wave. Section 5 is devoted to ord $\delta = \epsilon^4$, and contains discussions of numerical

as well as perturbation solutions of the governing equation. The paper concludes, in § 6, with an analysis of the situation ord $\delta < \epsilon^4$.

Finally, we should list the limitations of the theory: account is taken of only one non-equilibrium process (transport phenomena are neglected), and this paper ignores the influences of lift, aircraft manoeuvres and atmospheric non-uniformities.

## 2. Conservation equations

The notation used in this paper is virtually identical to that in I; so we shall avoid repeating minor points. The dimensionless governing equations for the steady non-equilibrium flow of a gas in the absence of molecular transport are

$$\mathbf{V}.\nabla\rho+\rho\nabla.\mathbf{V}=0, \tag{2.1}$$

$$\rho\mathbf{V}.\nabla\mathbf{V}+\nabla p=0, \tag{2.2}$$

$$\mathbf{V}.\nabla p+\rho a_f^2(\nabla.\mathbf{V}+\sigma\mathbf{V}.\nabla q)=0, \tag{2.3}$$

$$\lambda\mathbf{V}.\nabla q=M_{f_0}(q_e-q), \tag{2.4}$$

$$h=h(p,T,q), \quad q_e=q_e(p,s). \tag{2.5), (2.6}$$

Two of the differential equations can be replaced by the important characteristic equations (e.g. Hayes & Probstein 1966, p. 538):

$$\frac{D_f^{\pm}p}{Dx}\pm\frac{\rho V^2}{\beta_f}\frac{D_f^{\pm}\theta}{Dx}+\frac{\cos\mu_f\tan^2\mu_f}{\cos(\theta\pm\mu_f)}\left(pV^2\frac{\sin\theta}{r}+\frac{VW}{a_f^2}\right)=0, \tag{2.7a, b}$$

$$\frac{D_f^{\pm}}{Dx}=\frac{\partial}{\partial x}+\tan(\theta\pm\mu_f)\frac{\partial}{\partial r}. \tag{2.8}$$

The three vital parameters in our problem are given by the relations

$$r=\epsilon f(x), \quad \lambda=\tau' U'/L', \tag{2.9), (2.10}$$

$$\hat{\delta}=(a_{f_0}/a_{e_0})^2-1=[\sigma(\partial q_e/\partial p)_s]_0. \tag{2.11}$$

Equation (2.9) describes the body shape, and we shall regard $\epsilon$ as the basic small parameter; $\lambda$, $\lambda^{-1}$ and $\hat{\delta}$ will be measured against $\epsilon$, as discussed in §1. Obviously, the thermodynamic state of the undisturbed gas is independent of $\epsilon$, but for a given practical situation it will be clear how these parameters are related, and we should expect the solutions in different regimes of parameter space to 'match' across the boundaries between these regimes.

## 3. Linear theory

The first step in the analysis is the determination of the solution of the linearized problem; it is of intrinsic interest, and forms a basis for identifying regions of non-uniformity and for providing boundary conditions for the appropriate equations. The linear theory was first dealt with by Clarke (1961), and then by Li & Wang (1962), Kraiko (1966) and Sinai (1975, in terms of matched asymptotic expansions). We shall

therefore only quote the salient results here. Briefly, one finds that perturbations in all six dependent variables are of the same order in the mid-field limit, i.e.

$$\boldsymbol{\psi}(x,r;\epsilon) = \boldsymbol{\psi}^{(0)} + \epsilon^2\boldsymbol{\psi}^{(1)}(x,r) + O(\epsilon^4), \tag{3.1}$$

where
$$\boldsymbol{\psi} = (p,\rho,u,v,q,q_e)^{\mathrm{T}} \tag{3.2}$$

and
$$\boldsymbol{\psi}^{(0)} = (p_0/\rho_0 a_{f_0}^2, 1, M_{f_0}, 0, 1, 1)^{\mathrm{T}}. \tag{3.3}$$

For our purposes it will suffice to quote two asymptotic results derived in I for the axial velocity perturbation $u^{(1)}$:

$$u^{(1)} \sim \frac{-M_{f0}}{(2\beta_{f0}r)^{\frac{1}{2}}}\,\mathscr{W}(\xi)\,e^{-\mu r}\left[1 + O\left(\frac{\xi}{\beta_{f0}r}, \frac{\delta\xi}{\lambda}, \frac{r\delta\xi}{\lambda^2}\right)\right], \tag{3.4}$$

where
$$\mathscr{W}(x) = \frac{1}{2\pi}\int_0^x \frac{S''(y)\,dy}{(x-y)^{\frac{1}{2}}} \tag{3.5}$$

and
$$S = \pi f^2, \quad \xi = x - \beta_{f0}r, \quad \delta = M_{f0}^2\hat{\delta}/\beta_{f0}^2, \quad \mu = \beta_{f0}\delta/2\lambda. \tag{3.6}$$

Equation (3.4) evidently describes a near-frozen region where the non-equilibrium effects are confined to a simple exponential decay along the linearized frozen characteristics.

The second result, which does not appear to have been derived previously in the literature, is analogous to the large-time result obtained for the piston problem (Clarke 1965):

$$u^{(1)} \sim \frac{-M_{f0}}{(2\beta_{e0}r)^{\frac{1}{2}}}\int_0^\infty \mathscr{W}(y)\exp\left[-\frac{(\xi_e - y)^2}{4Br}\right]\frac{dy}{2(\pi Br)^{\frac{1}{2}}}\left[1 + O\left(\frac{\lambda}{\beta_{f0}r\delta}, \frac{|\xi_e|}{\beta_{f0}r\delta}\right)\right], \tag{3.7}$$

where
$$\left.\begin{aligned} B = \beta_{e0}\lambda\delta/2b^2, \quad b = \beta_{e0}/\beta_{f0}, \\ \xi_e = x - \beta_{e0}r, \quad \beta_{e0}^2 = M_{e0}^2 - 1, \quad M_* = V'/a_*' \quad (* = e,f). \end{aligned}\right\} \tag{3.8}$$

Sirovich (1968) and Chong & Sirovich (1970) analysed the problem for a viscous conducting gas instead of a relaxing one; they too determined the asymptotic values in the far field but their papers do not contain an expression similar to (3.7). Seeing that the process in both cases is one of dilatation, the existence of an equivalent bulk viscosity leads one to suspect that some manipulation of Chong & Sirovich's integrals might well lead to the form (3.7). Observe that a statement equivalent to (3.7) is

$$B\,\partial^2 w/\partial\xi_e^2 = \partial w/\partial r, \quad w(\xi_e, 0) = -M_{f0}(2\beta_{e0})^{-\frac{1}{2}}\,\mathscr{W}(\xi_e), \tag{3.9}$$

where
$$w = r^{\frac{1}{2}}u^{(1)}. \tag{3.10}$$

We are now in a position to analyse the nonlinear waves, and we shall find the near-frozen and near-equilibrium regimes amenable to calculations. In practice these domains are very far apart in physical space, and bridging can probably be achieved only by numerical techniques.

In the following sections we extend the results of I to encompass general, pointed, *smooth* bodies of revolution, and this means that besides $\epsilon$ and $\delta$ the role of $\lambda$ has to be accounted for.

## 4. Intermediate $\delta$

The phrase 'intermediate $\delta$' is taken to mean $1 \geqslant \operatorname{ord}\delta > \epsilon^4$; the reason for the critical size of $\delta$ being $\epsilon^4$ will transpire in the analysis (Sinai 1975; Clarke & Sinai 1977).

Before we continue let us define a quantity

$$\nu \equiv \lambda\epsilon^4/\delta. \tag{4.1}$$

### 4.1. *Near-frozen front*, $\operatorname{ord}\nu < 1$

Consider (3.4); if $\xi \ll 1$ we may approximate $\mathscr{W}$ by its value for small argument, which leads to

$$u \sim M_{f0} - \epsilon^2\pi^{-1}M_{f0}S''(0)\left(\frac{\xi}{2\beta_{f0}r}\right)^{\frac{1}{2}}\exp\left(-\frac{\beta_{f0}\delta r}{2\lambda}\right). \tag{4.2}$$

We may now follow exactly the same procedure as in I to show that the linear theory breaks down (in its ability to predict wavelet positions) when $\xi = O(\epsilon^4\lambda/\delta)$ with $r\delta/\lambda = O(1)$. In other words, the re-scaled co-ordinates should be

$$\Xi = \delta\xi/\lambda\epsilon^4, \quad R = \delta r/\lambda. \tag{4.3}$$

It is unnecessary for us to solve this problem formally; for, besides the results in I, there is ample evidence (e.g. Jones 1964; Wegener, Chu & Klikoff 1965; Blythe 1969; Ryzhov 1971; Chou & Chu 1971) to suggest that in those regions where high frequency convection is important one may apply the method variously described as the PLK or strained co-ordinates technique (Van Dyke 1975, p. 99) or the nonlinearization method (Whitham 1974, p. 312). If we label the nonlinear characteristics by $\alpha$ and invoke the relation (I, p. 509)

$$(\partial\xi/\partial r)_\alpha \simeq \epsilon^2\beta_{f0}^{-1}\Gamma_{f0}M_{f0}^3u^{(1)}, \tag{4.4}$$

where

$$\Gamma_f = a_f^{-1}[\partial(\rho a_f)/\partial\rho]_{s,q},$$

we can immediately deduce that when $\Xi$ and $R$ are $O(1)$

$$u \sim M_{f0} - \epsilon^2 M_{f0}\pi^{-1}S''(0)\,(\alpha/2\beta_{f0}r)^{\frac{1}{2}}\exp(-\mu r), \tag{4.5}$$

$$\xi = \alpha - \epsilon^2\Gamma_{f0}M_{f0}^4\beta_{f0}^{-2}S''(0)\,(\lambda\alpha/\pi\delta)^{\frac{1}{2}}\operatorname{erf}(\mu r)^{\frac{1}{2}}. \tag{4.6}$$

The analysis leading to (4.3) is vital, however, inasmuch as it indicates the permissible ranges of $\epsilon$, $\lambda$ and $\delta$ which are implied in (4.5) and (4.6): since we stipulated that $\xi \ll 1$, (4.3) requires

$$\operatorname{ord}(\lambda/\delta) < \epsilon^{-4}. \tag{4.7}$$

Using the weak shock fitting rule (Whitham 1974, p. 321), the shock locus is found from [see (3.6)]

$$\alpha_s^{\frac{1}{2}} = \tfrac{3}{4}l\operatorname{erf}(\mu r_s)^{\frac{1}{2}}, \tag{4.8}$$

$$\xi_s = \frac{-3}{16}l^2[\operatorname{erf}(\mu r_s)^{\frac{1}{2}}]^2 = \frac{-3}{16}\left(\frac{\lambda\epsilon^4}{\delta}\right)\frac{\Gamma_{f0}^2M_{f0}^8}{\pi\beta_{f0}^4}[S''(0)\operatorname{erf}(\mu r_s)^{\frac{1}{2}}]^2, \tag{4.9}$$

where

$$l = \epsilon^2\beta_{f0}^{-\frac{3}{2}}(2\pi\mu)^{-\frac{1}{2}}\Gamma_{f0}M_{f0}^4S''(0) \tag{4.10}$$

and the subscript $s$ denotes values on the frozen discontinuity. This has a bearing on the interesting result derived by Chou & Chu (1971), who deduced (as do we) that the

shape and strength of the frozen discontinuity emanating from the tip depend only on the tip angle. However, Chou & Chu concluded that this phenomenon occurs when $\lambda = O(\delta)$, and the present theory indicates that the 'decay length' $\lambda/\delta$ is permitted to lie in the far greater range dictated by (4.7).

The determination of the shock strength and of the relaxation zone behind the discontinuity are described in I.

Near-frozen conditions may be expected to arise wherever the body profile is not sufficiently smooth, and partly dispersed shocks will therefore appear downstream of the bow shock; this is an interesting feature of the problem which merits further study, but it will not be pursued in the present paper. We confine ourselves to the conjecture that the characteristic-parameter (or strained co-ordinates) method, which is the one employed by Clarke (1965), Chou & Chu (1971) and Chou (1972), may be valid in such regions.

In conclusion we point out that when the specific process under consideration is vibrational relaxation, $\lambda$ is normally so small that the inequality (4.7) is easily satisfied.

### 4.2. *Near-frozen flow*, ord $(\lambda\epsilon^4/\delta) \geqslant 1$

When ord $\nu \geqslant 1$ we observe from (4.3) that $\xi$ is no longer small, and we are forbidden to employ the small-argument asymptotic expression for $\mathscr{W}$. We could retain the exact $\mathscr{W}$ but that would lead to algebraic complexity when ord $\nu = 1$ and to large-argument asymptotics of $\mathscr{W}$ when ord $\nu > 1$. Moreover, (4.3) gives the false impression that the breakdown region moves away from the body as $\lambda \to \infty$; in fact we know that in the frozen limit the non-uniformity arises where $\xi = \text{ord } 1$ and $r = \text{ord } \epsilon^{-4}$ (Landahl & Lofgren 1973; Sinai 1975). A more satisfactory treatment can therefore be achieved by looking at the latter region together with a careful assessment of the rate equation; this will lead to a Varley–Rogers equation (Varley & Rogers 1967) with a term proportional to $\lambda^{-1}$, and the Varley–Rogers equation itself will transform into the one governing classical frozen flow as $\lambda \to \infty$.

The new co-ordinates are therefore $\xi$ and $R$, where

$$R = \epsilon^4 r. \tag{4.11}$$

Let us write

$$\boldsymbol{\psi}(\xi, R) = \boldsymbol{\Psi}^{(0)} + \mathbf{G}(\epsilon)\,\boldsymbol{\Psi}^{(1)}(\xi, R) + \ldots, \tag{4.12}$$

where

$$G_{ij} = \Delta_{\psi}(\epsilon)\,\delta_{ij}, \tag{4.13}$$

$\delta_{ij}$ is the Kronecker delta and $\Delta_{\psi}$ is the gauge function associated with the dependent variable $\boldsymbol{\psi}$. It is easily shown that

$$\Delta_p = \Delta_\rho = \Delta_u = \Delta_v = \Delta_{q_e} = \epsilon^4 \tag{4.14}$$

and the rate equation (2.4) shows that a consistent formulation can materialize only if

$$\Delta_q = \epsilon^4/\lambda. \tag{4.15}$$

In fact since ord $\nu \geqslant 1$, ord $\Delta_q \leqslant \epsilon^8/\delta$. The momentum and continuity equations show that

$$M_{f0} R^{(1)} = \beta_{f0} V^{(1)} - U^{(1)}, \quad V^{(1)} = -\beta_{f0} U^{(1)}, \quad P^{(1)} = -M_{f0} U^{(1)}, \tag{4.16}$$

(2.4) yields

$$Q_{\xi}^{(1)} = Q_e^{(1)} + O(\lambda^{-1}) \tag{4.17}$$

and the perturbation in the equilibrium value of $q$ is

$$Q_e^{(1)} = [(\partial q_e/\partial p)_s]_0 P^{(1)}. \tag{4.18}$$

In employing (2.7) it is necessary to use the following expression for the slope of the frozen characteristics:

$$\tan(\theta \pm \mu_f) = (a_f^2 - v^2)[\pm a_f(V^2 - a_f^2)^{\frac{1}{2}} - uv]^{-1}. \tag{4.19}$$

An equation for $U^{(1)}$ can be found by employing the entropy relation (see I), (2.7$a$), (2.8) and (2.11) and all of (4.14)–(4.19). This yields

$$K_f U^{(1)} U_\xi^{(1)} + 2U_R^{(1)} + R^{-1}U^{(1)} + \beta_{f0}(\delta/\lambda\epsilon^4)\, U^{(1)} = 0, \tag{4.20}$$

where

$$K_f = 2\Gamma_{f0} M_{f0}^3/\beta_{f0}. \tag{4.21}$$

Since the second-order term in the frozen far field is $O(\epsilon^8)$ (Landahl & Lofgren 1973) we adopt the view that the last term in (4.20) is truly negligible when ord $(\lambda\epsilon^4/\delta) \geqslant \epsilon^{-4}$. The parametric solution of (4.20) is

$$R^{\frac{1}{2}} U^{(1)} = H(\alpha) \exp(-\beta_{f0} R\delta/2\lambda\epsilon^4), \tag{4.22}$$

where the parameter $\alpha$ is determined from

$$\xi = G(\alpha) + \tfrac{1}{2} H(\alpha)\, K_f (2\pi\lambda\epsilon^4/\beta_{f0}\delta)^{\frac{1}{2}} \operatorname{erf}(\beta_{f0} R\delta/2\lambda\epsilon^4)^{\frac{1}{2}}. \tag{4.23}$$

The arbitrary functions $G$ and $H$ must be chosen so as to satisfy the matching requirements; these are found by substituting (4.11) in (3.4) and (3.1) and taking the limit $\epsilon \to 0$ with $\xi$ and $R$ fixed. It transpires that $U^{(1)}$ should satisfy the condition

$$U^{(1)}(\xi, R \downarrow 0) \sim -M_{f0}(2\beta_{f0} R)^{-\frac{1}{2}} \mathscr{W}(\xi). \tag{4.24}$$

On comparing (4.22) with (4.24) it is clear that

$$H(\alpha) = -M_{f0}(2\beta_{f0})^{-\frac{1}{2}} \mathscr{W}(\alpha). \tag{4.25}$$

It is also apparent from (4.23) that since we wish to identify $\alpha$ with $\xi$ as $R \downarrow 0$,

$$G(\alpha) = \alpha \tag{4.26}$$

and (4.23) becomes

$$\xi = \alpha - \epsilon^2 \Gamma_{f0} M_{f0}^4 \beta_{f0}^{-2} (\pi\lambda/\delta)^{\frac{1}{2}} \mathscr{W}(\alpha) \operatorname{erf}(\beta_{f0}\delta r/2\lambda)^{\frac{1}{2}}. \tag{4.27}$$

As expected, the solution has turned out to be a generalization of (4.4) and (4.5), the classical frozen result (Whitham 1952) being recovered as $\lambda \to \infty$. The loci and strengths of frozen discontinuities are determined from

$$k_1 \operatorname{erf}\left(\frac{\beta_{f0}\delta r_s}{2\lambda}\right)^{\frac{1}{2}} = \left[\frac{\alpha_2 - \alpha_1}{\mathscr{W}(\alpha_2) - \mathscr{W}(\alpha_1)}\right], \tag{4.28}$$

$$2\int_{\alpha_1}^{\alpha_2} \mathscr{W}(y)\, dy = (\alpha_2 - \alpha_1)[\mathscr{W}(\alpha_2) + \mathscr{W}(\alpha_1)], \tag{4.29}$$

where

$$k_1 = \epsilon^2 \Gamma_{f0} M_{f0}^4 \beta_{f0}^{-2} (\pi\lambda/\delta)^{\frac{1}{2}}. \tag{4.30}$$

### 4.3. *Equilibrium wave*, ord $(\lambda\delta) > \epsilon^4$

The near-frozen analysis has concentrated on regions where $\delta r/\lambda$ for ord $(\lambda\epsilon^4) < \delta$, or $\epsilon^4 r$ for ord $(\lambda\epsilon^4) \geqslant \delta$, is $O(1)$. When $\delta r/\lambda$ is large (3.7) is the relevant linear estimate, and low frequency convection is evidently important.

We could attempt to use the linear theory to estimate the wavelet shapes; this is done by invoking (4.19) with the subscript $f$ replaced by $e$ and by following elementary thermodynamic manipulations:

$$\left(\frac{\partial\xi_e}{\partial r}\right)_\alpha \simeq \epsilon^2 \Gamma_{e0} M_{e0}^4 u^{(1)}/M_{f0}\beta_{e0}. \tag{4.31}$$

However, substitution of (3.7) effectively leaves us with an unwieldy integro-differential equation for $\xi_e$ as a function of $r$ on the curves $\alpha =$ constant. We shall therefore follow a formal and less awkward procedure as follows. If we introduce the general stretching

$$\Xi = \Delta_{\xi_e}\xi_e, \quad R = \Delta_r r, \tag{4.32}$$

we may focus our attention on a far field by insisting that $\xi_e \ll r$, i.e.

$$\Delta_r \ll \Delta_{\xi_e}. \tag{4.33}$$

Substituting (4.32) and (4.33) in the governing equations, it immediately follows that [see (4.13)]

$$\Delta_p = \Delta_\rho = \Delta_u = \Delta_v = \Delta_{q_e} \equiv \Delta, \tag{4.34}$$

$$M_{f0}R^{(1)} = \beta_{e0}V^{(1)} - U^{(1)}, \quad P^{(1)} = -M_{f0}U^{(1)}, \quad V^{(1)} = -\beta_{e0}U^{(1)}. \tag{4.35}$$

Turning now to the rate equation, we are at present interested in those regions of the far field where conditions are close to equilibrium, and we therefore insist that

$$\Delta_q = \Delta, \quad \Delta_{\bar{q}} = o(\Delta), \quad \bar{q} = q - q_e. \tag{4.36}$$

It then follows from (2.4) that

$$\Delta_{\bar{q}} = \lambda\Delta\Delta_{\xi_e}, \quad \bar{Q}^{(1)} = [M_f(\partial q_e/\partial p)_s]_0 U_\Xi^{(1)}. \tag{4.37}$$

Equation (4.36) implies that all thermodynamic quantities can be evaluated at the local equilibrium state with a relative order $\Delta_{\bar{q}}$, i.e.

$$\mathbf{V}.\nabla p + \rho a_e^2(\nabla.\mathbf{V} + \sigma_e \mathbf{V}.\nabla\bar{q}) \simeq 0. \tag{4.38}$$

This equation may also be deduced from the expression given by Ryzhov (1971):

$$\frac{Dp}{Dt} + \rho a_e^2 \nabla.\mathbf{V} = \left(\frac{\partial p}{\partial Q}\right)_{\rho,s}\frac{DQ}{Dt} - \frac{Q}{T}\left(\frac{\partial p}{\partial s}\right)_{\rho,Q}\frac{Dq}{Dt},$$

where $Q = (\partial h/\partial q)_{p,s}$. Clearly (2.7$a$, $b$) now apply with the subscripts $f$ replaced by $e$, and with

$$W = (\rho a^2\sigma)_e \mathbf{V}.\nabla\bar{q}. \tag{4.39}$$

Moreover, these two equations indicate that

$$\Delta = \Delta_r/\Delta_{\xi_e} \tag{4.40}$$

and

$$\lambda\delta\Delta_{\xi_e}\Delta_r = \Delta\Delta_r,$$

i.e.

$$\Delta_{\xi_e} = \Delta/\lambda\delta, \quad \Delta_r = \Delta^2/\lambda\delta \tag{4.41$a$}$$

and

$$\Delta_{\bar{q}} = \Delta^2/\delta. \tag{4.41$b$}$$

In passing we note two facts: first, that $\Delta$ is as yet unknown and will be determined during the matching process; second, that (3.7) can be rewritten as

$$u^{(1)} \sim \frac{-M_{f0}}{(2\pi\beta_{e0}r)^{\frac{1}{2}}}\int_0^\infty \mathscr{W}(A_1 y)\exp\left[-(\zeta_e - y)^2\right]dy, \tag{4.42}$$

where
$$\zeta_e = \xi_e(2b^{-2}\beta_{e0}\lambda\delta r)^{-\frac{1}{2}}, \quad A_1 = (4Br)^{\frac{1}{2}}. \tag{4.43}$$

In view of all that has been said, we define the new co-ordinates by

$$\Xi = \Delta\xi_e/\lambda\delta, \quad R = \Delta^2 r/\lambda\delta. \tag{4.44}$$

In order to place subsequent work in this section in perspective, let us apply the matching rule before we derive the governing equation. Writing the far-field series again as in (4.12) and (4.13), we wish to find a boundary condition on $U^{(1)}$; substituting (4.44) in (4.42) gives

$$u^{(1)} \sim \frac{-M_{f0}}{(2\pi\beta_{e0})^{\frac{1}{2}}}\left(\frac{\Delta^2}{\lambda\delta R}\right)^{\frac{1}{2}}\int_0^\infty \mathscr{W}\left(cR^{\frac{1}{2}}\frac{\lambda\delta}{\Delta}y\right)\exp\left[-\left(\frac{\Xi}{cR^{\frac{1}{2}}}-y\right)^2\right]dy, \tag{4.45}$$

where
$$c = (2b^{-2}\beta_{e0})^{\frac{1}{2}}. \tag{4.46}$$

The assumption ord $(\lambda\delta) > \Delta$ is in fact implicit in (4.44) because in the limit $\lambda \to 0$ breakdown occurs where $\xi_e = O(1)$ and $r = O(\epsilon^{-4})$, in the same way that an analogous breakdown occurs in the frozen limit (see § 4.1). We therefore need the asymptotic behaviour of $\mathscr{W}(x)$ as $x \to \infty$:

$$\mathscr{W}(x) \sim \frac{S'(1)}{2\pi x^{\frac{1}{2}}} + \frac{S'(1)-S(1)}{4\pi x^{\frac{3}{2}}} + O(x^{-\frac{5}{2}}). \tag{4.47}$$

It is not unusual for $\mathscr{W}$ to decay faster than $x^{-\frac{3}{2}}$ if the body is finite; for example, if $f(1) = 0$ then $S(1) = 0 = S'(1)$. Clearly, $\mathscr{W} \sim x^n$ with $n \leqslant -\frac{1}{2}$ if the body is finite, but in order to include semi-infinite bodies in our analysis, let us write

$$\mathscr{W}(x \to \infty) \sim x^n \tag{4.48}$$

on the understanding that $n \leqslant \frac{1}{2}$ ($\frac{1}{2}$ corresponds to the cone, and we cannot allow the body to grow faster than the cone as $x \to \infty$). Substituting (4.48) in (4.45) we find that if $n > 0$

$$\Delta = \lambda\delta[\epsilon^2(\lambda\delta)^{-\frac{1}{2}}]^{1/n}. \tag{4.49}$$

However, when the body is finite, so that $S''(x)$ vanishes when $x > 1$, we find that $\Delta = \lambda\delta/\epsilon^4$; seeing that $\lambda\delta$ can be $O(1)$, this result is patently inadmissible, and the matching rule indicates that the linear theory is valid in the present region (evidently the diffusivity $B$ is sufficiently large for the nonlinear effects to be relatively unimportant). These conclusions are analogous to Blythe's (1969) deductions for the piston problem, although he did not consider the implications of $\lambda$ and $\delta$ taking on extreme values in the 'intermediate $\delta$' context, except for allowing $\lambda$ to be large. Observe that since $0 < n \leqslant \frac{1}{2}$, $1 - 1/2n < 0$ and (4.44) and (4.49) still apply as $\lambda \to \infty$; this domain of non-uniformity is simply shifted away from the body as $\lambda$ increases, although the near-frozen results of § 4.2 then apply in the 'usual' far field.

Using equation (8) of I, the perturbation to the equilibrium sound speed is found to be

$$A_e^{(1)} = M_{f0}M_{e0}^{-1}(\Gamma_{e0} - 1)\,U^{(1)}, \tag{4.50}$$

where
$$\Gamma_e = a_e^{-1}[\partial(\rho a_e)/\partial\rho]_s. \tag{4.51}$$

The equilibrium form of (4.19) then shows that

$$\frac{D_e^{\pm}}{Dx} = \frac{\Delta}{\lambda\delta}\frac{\partial}{\partial\Xi} \pm \frac{1}{\beta_{e0}}[1 - K^{\pm}U^{(1)}]\left(-\beta_{e0}\frac{\Delta}{\lambda\delta}\frac{\partial}{\partial\Xi} + \frac{\Delta^2}{\lambda\delta}\frac{\partial}{\partial R}\right), \tag{4.52}$$

where

$$K^{\pm} = M_{f0}^{-1}M_{e0}^2(\Gamma_{e0}\beta_{e0}^{-2}M_{e0}^2 - 1 \pm 1)\Delta. \tag{4.53}$$

Invoking (2.7*a*), (4.35), (4.37) and (4.52) we finally derive an axisymmetric version of Burgers' equation:

$$K_e U^{(1)}U_{\Xi}^{(1)} + 2U_R^{(1)} + R^{-1}U^{(1)} = \beta_{e0}^{-1}\beta_{f0}^2 U_{\Xi\Xi}^{(1)}, \tag{4.54}$$

where

$$K_e = 2M_{f0}^{-1}\beta_{e0}^{-1}\Gamma_{e0}M_{e0}^4. \tag{4.55}$$

Equation (4.45) provides a boundary condition; $U^{(1)}$ should behave like

$$\frac{-M_{f0}c^n}{(2\pi\beta_{e0})^{\frac{1}{2}}}R^{-\frac{1}{2}(1-n)}\int_0^{\infty} y^n \exp\left[-\left(\frac{\Xi}{cR^{\frac{1}{2}}} - y\right)^2\right]dy \tag{4.56}$$

as $R \downarrow 0$ with $\Xi R^{-\frac{1}{2}}$ fixed ($0 < n \leqslant \frac{1}{2}$).

As far as can be ascertained, no exact analytical solution of the axisymmetric Burgers equation has yet been published. Parker (1975) has applied the Cole–Hopf transformation (e.g. Lighthill 1956) to a general class of equations and obtained a spatially dependent diffusivity multiplying a logarithmic term (Leibovich & Seebass 1974, p. 124); subsequent linearization of this term allowed him to obtain closed-form solutions. The need to match $U^{(1)}$ with the mid-field result unfortunately invalidates this procedure in the present case; in fact, Parker's solution is apparently unable to satisfy a singular boundary condition involving terms like $R^{-m}$, $m > 0$ (Sinai 1975).

Mention should also be made of similarity solutions, but we shall postpone such a discussion until the next section, where it will be more relevant.

Let us digress on the matching procedure [cf. (4.45)]. Specifically, we shall try to answer the following question: why does the diffusivity $\lambda\delta$ have a critical size $O(\epsilon^4)$? It has already been shown that, when ord $(\lambda\delta)$ is greater than the initially unknown $\Delta$, $\Delta$ turns out to depend on the body shape. Now consider a situation where

$$\text{ord}\,(\lambda\delta) \leqslant \Delta.$$

Here we need to use the asymptotic behaviour of $\mathscr{W}$ for *small* argument, namely $\mathscr{W}(x) \sim x^{\frac{1}{2}}$, and it transpires that $\Delta = \epsilon^4$ and hence ord $(\lambda\delta) \leqslant \Delta$ if ord $(\lambda\delta) \leqslant \epsilon^4$. These thoughts are further consolidated by (4.49), for it confirms that ord $(\lambda\delta) > \Delta$ when ord $(\lambda\delta) > \epsilon^4$ provided only that $n > 0$. In addition to these arguments we know (as has been mentioned before) that when $\lambda = 0$ breakdown occurs where $\xi_e =$ ord 1 and $r =$ ord $\epsilon^{-4}$ [consult the pertinent comments above (4.11)].

### 4.4. *Equilibrium wave,* ord $(\lambda\delta) \leqslant \epsilon^4$

Let us define the quantity

$$\nu^* \equiv \lambda\delta/\epsilon^4 \leqslant \text{ord } 1. \tag{4.57}$$

In view of the aforementioned, a study of the ord $(\nu^*) \leqslant 1$ situation will be facilitated by examining the region in which $\xi_e = O(1)$ and $r = O(\epsilon^{-4})$, i.e. the new independent variables should be $\xi_e$ and $R$, where

$$R = \epsilon^4 r. \tag{4.58}$$

It transpires that

$$\Delta_p = \Delta_\rho = \Delta_u = \Delta_v = \Delta_{q_e} = \epsilon^4, \tag{4.59}$$

and this time the rate equation indicates that

$$\Delta_q = \epsilon^4, \quad \Delta_{\tilde{q}} = \lambda\epsilon^4. \tag{4.60}$$

Observe that since ord $(\lambda\delta) \leqslant \epsilon^4$, ord $(\Delta_{\tilde{q}}) \leqslant \epsilon^8/\delta$. The subsequent analysis is almost identical to that in the previous section, and $U^{(1)}$ is found to satisfy an equation which is barely (but usefully) different from (4.54):

$$K_e U^{(1)} U^{(1)}_{\xi_e} + 2U^{(1)}_R + R^{-1}U^{(1)} = (\lambda\delta/\epsilon^4)\beta_{e0}^{-1}\beta_{f0}^2 U^{(1)}_{\xi_e\xi_e}. \tag{4.61}$$

Again, the diffusive term on the right-hand side is deemed negligible when

$$\text{ord}\,(\lambda\delta/\epsilon^4) \leqslant \epsilon^4.$$

The reasons why (4.61) is considered more useful than (4.54) are twofold. First, (4.61) is susceptible to perturbation techniques when ord $\nu^* < 1$, and this inequality is normally satisfied in the context of vibrational relaxation in the atmosphere. Second, it transpires that the boundary condition on (4.61) is a much simpler one than (4.56). In fact, the matching condition corresponds to classical equilibrium requirements, as can be verified by direct manipulations or by invoking the properties of the Dirac delta function; hence

$$U^{(1)}(\xi_e, R \downarrow 0) \sim -M_{f0}(2\beta_{e0}R)^{-\frac{1}{2}}\mathscr{W}(\xi_e). \tag{4.62}$$

Write

$$w = R^{\frac{1}{2}}U^{(1)}. \tag{4.63}$$

Then

$$K'_e R^{-\frac{1}{2}} w w_{\xi_e} + w_R = \mu^* w_{\xi_e\xi_e}, \tag{4.64}$$

where

$$K'_e = \tfrac{1}{2}K_e, \quad \mu^* = \lambda\delta\beta_{f0}^2/2\beta_{e0}\epsilon^4. \tag{4.65}$$

Let us find perturbation solutions to (4.64) in the practically relevant case ord $\nu^* < 1$ (Hodgson & Johannesen 1971). Equation (4.61) is immediately recognized as a singular perturbation problem (Cole 1968; Murray 1968; Van Dyke 1975); initially we seek an 'outer' solution of the form

$$w = w^{(0)} + \mu^* w^{(1)} + o(\mu^*) \tag{4.66}$$

and we find, with the aid of (4.62), that

$$w^{(0)} = F(\beta) = -M_{f0}(2\beta_{e0})^{-\frac{1}{2}}\mathscr{W}(\beta), \quad \xi_e = \beta + K_e F(\beta) R^{\frac{1}{2}}, \tag{4.67}$$

$$w^{(1)} = \frac{F''(\beta)}{2[K'_e F'(\beta)]^2}(\ln T + T^{-1} - 1) = \frac{2(2\beta_{e0})^{\frac{1}{2}}\mathscr{W}''(\beta)}{M_{f0}K_e^2\mathscr{W}'^2(\beta)}(1 - T^{-1} - \ln T), \tag{4.68}$$

where

$$T = 1 + K_e F'(\beta) R^{\frac{1}{2}} \equiv (\partial\xi_e/\partial\beta)_R. \tag{4.69}$$

The breakdown is highlighted in (4.68); $T$ vanishes on the envelopes of the characteristics $\beta$ = constant, i.e. breakdown occurs near the shock waves. Be that as it may, we can locate the shock waves (with an error $O(\mu^*)$) by the standard techniques, and values of $w$ ahead of and behind these equilibrium shocks, denoted by $W_f$ and $W_R$, will be required during the 'inner' calculation for the shocks' structures. Writing the inner expansion as

$$w(\eta, R) = W^{(0)} + \mu^* W^{(1)} + o(\mu^*), \tag{4.70}$$

where

$$\eta = [\xi_e - \theta(R)]/\mu^* \tag{4.71}$$

and $\theta(R)$ is the value of $\xi_e$ along the shock calculated from (4.67), we derive an equation which has appeared in similar form several times in the literature:

$$\tfrac{1}{2}K_e R^{-\frac{1}{2}} W^{(0)} W_\eta^{(0)} - (d\theta/dR)\, W_\eta^{(0)} - W_{\eta\eta}^{(0)} = 0. \tag{4.72}$$

Integrating twice and applying the conditions $W^{(0)} = W_f$ and $W_\eta = 0$ as $\eta \to -\infty$ and $W^{(0)} = W_R$ and $W_\eta = 0$ as $\eta \to \infty$, we find that

$$\frac{d\theta}{dR} = \frac{K_e'}{2R^{\frac{1}{2}}}(W_f + W_R), \tag{4.73}$$

$$\frac{K_e}{4R^{\frac{1}{2}}}(W_f - W_R)\,\eta = \ln\left(\frac{W_f - W^{(0)}}{W^{(0)} - W_R}\right) + H(R), \tag{4.74a}$$

or

$$\frac{W_f - W^{(0)}}{W^{(0)} - W_R} = \exp\left[\frac{K_e(W_f - W_R)(\xi_e - \theta)}{R^{\frac{1}{2}}\mu^*} - H\right], \tag{4.74b}$$

where $H$ is an undetermined function (assumed to be $O(1)$). Equation (4.73) is no more than the 'mean wavelet direction' condition for weak shocks (e.g. Whitham 1952), and (4.74$a$, $b$) correspond to the classical, Taylor, diffusion-resisted structure (e.g. Lighthill 1956, p. 287), with the shock thickness (defined in the usual way) proportional to a diffusivity and inversely proportional to the velocity change across it. In fact, comparison of (4.74$b$) with the classical result indicates that the dimensional diffusivity $\delta^*$ is given by

$$\delta^* = U'L'\lambda\delta\beta_{f0}^2/M_{e0}^4 = \tau_0' U'^2 \beta_{f0}^2 \delta/M_{e0}^4 = \tau_0' \hat{\delta} a_{e0}^4/a_{f0}^2. \tag{4.75}$$

It should be noted that in any compression wave $W_f > W^{(0)} > W_R$. At sufficiently large $R$ the viscous region will engulf the whole Mach zone, as pointed out by Chong & Sirovich (1973; see also Sanchez-Palencia-Hubert 1976). If we denote the dimensional widths of the shock and Mach zones by $\delta_s'$ and $\delta_m'$ respectively, we know from previous considerations and the classical Whitham theory that at sufficiently large distances

$$\delta_s' \sim \delta^*(r'/L')^{\frac{3}{4}}/\epsilon^2 U', \quad \delta_m' \sim \epsilon L'(r'/L')^{\frac{1}{4}}. \tag{4.76}$$

Like Chong & Sirovich we declare that the viscous and inviscid zones may not be regarded as 'separate' for radii larger than that at which $\delta_s' = O(\epsilon\delta_m')$, i.e. when

$$r'/L' = O(\epsilon^8 R_R^2), \tag{4.77}$$

where (in our case) $R_R$ is a 'relaxation Reynolds number' given by

$$R_R = U'L'/\delta^* = M_{e0}^4/\beta_{f0}^2\lambda\delta. \tag{4.78}$$

It should be observed that when $R_R$ is not larger than $O(\epsilon^{-4})$ the critical $r'/L'$ is not large; this may well be related to the comments made at the end of §4.3, and (4.77) constitutes another pointer at $\epsilon^4$ as the critical order of magnitude of the diffusivity. These thoughts are related to the 'lobe Reynolds number' discussed by Lighthill (1956, p. 333) and Leibovich & Seebass (1974, p. 120).

We can assess the importance of relaxation in the present region by comparing the equivalent bulk (kinematic) viscosity $\delta^*$ with the shear viscosity $\nu_s$ of air. Let us assume the following typical values for the parameters:

$$a_{e0} = 300\,\mathrm{m/s}, \quad \hat{\delta} = 10^{-4}, \quad \nu_s = 10^{-4}\,\mathrm{m^2/s}.$$

Substituting in (4.75) gives

$$\delta^*/\nu_s \simeq 10^5 \tau_0' \tag{4.79}$$

with $\tau_0'$ expressed in seconds. Since (e.g. Hodgson & Johannesen 1971; Sutherland 1975) $\tau_0'$ varies typically in the range $10^{-3}$s (dry conditions) to $10^{-6}$s (humid conditions), we see that in some atmospheric environments the equivalent bulk viscosity can overwhelm the shear viscosity (Lighthill 1956, p. 281); under such circumstances omission of $\delta^*$ leads to gross under-estimation of the shock rise times. These results provide the information we sought regarding the detailed structure of the $N$-wave.

Let us now turn to the matter of similarity solutions of (4.64). Sinai (1976) found a body satisfying the similitude requirements in terms of the grouping $\xi_e R^{-\frac{1}{2}}$, but that calculation was carried out in the equilibrium limit $\lambda \to 0$ with $\delta$ small, i.e. ord $\delta = \epsilon^4$. However, the matching condition (4.62) is identical to the one implemented by Sinai, and we therefore conclude that the solution discussed in that paper is relevant under the present circumstances as well, due care being taken to account for the different coefficients in Burgers' equation (these differences are negligible when $\delta$ is small).

## 5. Small $\delta$

The phrase 'small $\delta$' implies that ord $\delta = \epsilon^4$; under such circumstances the source term in (2.7) undergoes a vital change in character, resulting in an equation which is less tractable than those encountered so far. Before continuing, let us define

$$A = \delta/\epsilon^4, \quad \hat{A} = \hat{\delta}/\epsilon^4. \tag{5.1}$$

### 5.1. *The case* ord $\lambda = 1$

It was pointed out in I that when $\delta$ is as small as $O(\epsilon^4)$ the mid-field result is the familiar frozen estimate,

$$u^{(1)} \sim -M_{f0}(2\beta_{f0}r)^{-\frac{1}{2}}\mathscr{W}(\xi), \tag{5.2}$$

provided only that $\xi \ll r$. Breakdown therefore again occurs where $\xi = O(1), r = O(\epsilon^{-4})$, and the co-ordinates defined in §4.2 apply directly, as do (4.14) and (4.16). Unlike the previous cases, the thermodynamic state in the far field is neither nearly frozen nor close to equilibrium, and according to (2.4) and (2.11)

$$\Delta_q = \epsilon^4, \tag{5.3}$$

$$\lambda Q_\xi^{(1)} + Q^{(1)} = -(\beta_{f0}^2\delta/M_{f0}\sigma_0)\,U^{(1)}. \tag{5.4}$$

Subsequent calculations follow those in §4.2 very closely, and (2.7$a$) leads to

$$K_f U^{(1)}U_\xi^{(1)} + 2U_R^{(1)} + R^{-1}U^{(1)} = (M_{f0}\sigma_0/\beta_{f0}\epsilon^4)\,Q_\xi^{(1)}. \tag{5.5}$$

Equations (5.4) and (5.5) may be combined to yield

$$(\lambda\,\partial/\partial\xi + 1)\,\mathscr{L}_f U^{(1)} + A\beta_{f0}U_\xi^{(1)} = 0, \tag{5.6}$$

where $\mathscr{L}_f$ is the familiar differential operator

$$\mathscr{L}_f = K_f U^{(1)}\partial/\partial\xi + 2\,\partial/\partial R + R^{-1}. \tag{5.7}$$

Equation (5.6) describes an axially symmetric flow which is analogous to the small-energy problems considered by Blythe (1969), Ockendon & Spence (1969), Ryzhov (1971) and Rudenko *et al.* (1974). Unfortunately no analytical solutions of these equations are known as yet. Blythe (1969) presented numerical solutions of the

small-$\delta$ (piston problem) equation for the *expansive* case; in our case the front is essentially compressive, but we shall postpone our discussion of numerical solutions of (5.6) until a subsequent section. A significant contribution to an understanding of the general features of the small-$\delta$ equation was made by Blythe, who studied the equation's characteristic form. Clarke & Sinai (1977) used certain features of the same technique, although the changed geometry alters the details somewhat, and the calculation set out below hardly differs from the corresponding analysis in that paper (we confine our attention to the front, or bow, shock).

First, transforming the variables via

$$X = \xi/\lambda, \quad Y = (A\beta_{f0}R/2\lambda)^{\frac{1}{2}}, \quad w = K_f(R/2A\beta_{f0}\lambda)^{\frac{1}{2}}\,U^{(1)}, \tag{5.8}$$

we find that $w$ satisfies the following parameter-free equation:

$$(\partial/\partial X + 1)(2ww_X + w_Y) + 2Yw_X = 0. \tag{5.9}$$

This equation's characteristics are $Y$ = constant (which approximate the streamlines) and $\alpha$ = constant (which approximate the nonlinear frozen Mach wavelets), where

$$(\partial X/\partial Y)_\alpha = 2w. \tag{5.10}$$

Application of what may be called the Von Mises transformation, with the aid of (5.10), leads to an equation for $X$ as a function of $\alpha$ and $Y$:

$$X_{\alpha YY} + X_\alpha X_{YY} + 2YX_{\alpha Y} = 0. \tag{5.11}$$

If we identify $\alpha$ with $\xi$ on $Y = 0$, the integral of (5.10) is

$$X = \frac{\alpha}{\lambda} + 2\int_0^Y w(\alpha, y)\,dy \tag{5.12}$$

and the matching condition (4.24), together with (5.8) and (5.10), translates into the following boundary condition:

$$X_Y(\alpha, 0) = -\tfrac{1}{2}K\lambda^{-\frac{1}{2}}\mathscr{W}(\alpha), \tag{5.13}$$

where

$$K = 2M_{f0}K_f/A^{\frac{1}{2}}\beta_{f0}. \tag{5.14}$$

Furthermore, (5.12) implies that

$$X(\alpha \leqslant 0, Y) = \alpha/\lambda, \quad X(\alpha > 0, 0) = \alpha/\lambda. \tag{5.15), (5.16}$$

For $\alpha$ small and positive, $X$ may be written as a series:

$$X = \sum_{n=1}^{\infty} \alpha^{\frac{1}{2}n} X_n(Y), \tag{5.17}$$

from which we find that

$$\xi = -\tfrac{1}{4}(\lambda\alpha/\pi)^{\frac{1}{2}}KS''(0)\operatorname{erf} Y + \alpha[1 + \Delta(Y)], \tag{5.18}$$

where $S''(0)$ is the limit of $S''(x)$ as $x$ decreases to zero from above, and

$$\Delta(Y) = \frac{K^2}{\pi^{\frac{3}{2}}}\left[\frac{S''(0)}{4}\right]^2 \int_0^Y \left[(y^2 - \tfrac{1}{2})\operatorname{erf} y + \frac{y}{\pi^{\frac{1}{2}}}\exp(y^2)\right]\exp(-y^2)\,dy. \tag{5.19}$$

The reader is referred to I for the pertinent comments regarding the behaviour of the head shock (we may assume, without loss of generality, that $S''(0) = 2\pi$).

The analysis which we have completed is admittedly of a limited nature; in addition to the restrictions on $\alpha$, we have not described the rear shock. However, the problem is a complex one, and we shall now content outselves with, first, a look at the behaviour for extreme $\lambda$, and second, numerical solutions of (5.6).

### 5.2. *The case* ord $\lambda < 1$

First, it is to be observed that, in terms of the linearized equilibrium characteristics $\xi_e$, (5.6) reads

$$\left(\lambda\frac{\partial}{\partial\xi_e}+1\right)[K_f U^{(1)}U^{(1)}_{\xi_e}+2U^{(1)}_R+R^{-1}U^{(1)}] = \lambda A\beta_{f0}U^{(1)}_{\xi_e\xi_e}+O(\delta). \tag{5.20}$$

Note too that, since ord $\delta = \epsilon^4$, $K_e = K_f$ to within our order of accuracy [see (4.21) and (4.55)].

It has already been pointed out that $\lambda$ is normally small; in their studies of this situation Blythe (1969), Ockendon & Spence (1969) and Rudenko *et al.* (1974) 'iterated' on their analogues of (5.6) to obtain Burgers' equation

$$K_f U^{(1)}U^{(1)}_{\xi_e}+2U^{(1)}_R+R^{-1}U^{(1)} = \lambda A\beta_{f0}U^{(1)}_{\xi_e\xi_e}+O(\lambda^2), \tag{5.21}$$

which is identical to (4.61) to $O(\delta)$. However, it was pointed out by Sinai (1975) and Crighton (1975, private communication) that Burgers' equation is invalid in certain regimes; in fact, (5.20) is a typical singular perturbation problem, the iterated equation yielding the 'outer' solution.

In the notation of §4.4, (5.20) can be written as

$$(\lambda\,\partial/\partial\xi_e+1)(K'_f R^{-\frac{1}{2}}ww_{\xi_e}+w_R) = \tfrac{1}{2}\beta_{f0}\nu^* w_{\xi_e\xi_e}. \tag{5.22}$$

It quickly follows that the outer solution is identical to (4.66), (4.67) and (4.68), with

$$\mu^* = \tfrac{1}{2}\beta_{f0}\nu^*. \tag{5.23}$$

In terms of the variables defined in (4.70) and (4.71), we find that the first inner term is governed by

$$K'_f R^{-\frac{1}{2}}W^{(0)}W^{(0)}_\eta - \frac{d\theta}{dR}W^{(0)}_\eta + \tfrac{1}{2}K'_f R^{-\frac{1}{2}}W^{(0)2} - \frac{d\theta}{dR}W^{(0)} = \tfrac{1}{2}A\beta_{f0}W^{(0)}_\eta + G(R). \tag{5.24}$$

Applying the upstream and downstream matching conditions, we find that (see §4.4)

$$\left.\begin{aligned} d\theta/dR &= \tfrac{1}{2}K'_f R^{-\frac{1}{2}}(W_f+W_R),\\ G(R) &= -\tfrac{1}{2}K'_f R^{-\frac{1}{2}}W_f W_R. \end{aligned}\right\} \tag{5.25}$$

An additional integration yields

$$(1-D)\ln[W_f-W^{(0)}]+(1+D)\ln[W^{(0)}-W_R] = -\eta+H(R), \tag{5.26}$$

where

$$D = 2A\beta_{f0}R^{\frac{1}{2}}/K_f(W_f-W_R). \tag{5.27}$$

Relations like (5.26) have appeared numerous times in the literature; specifically, the wave is *partly* dispersed wherever $R^{-\frac{1}{2}}(W_f-W_R)$ is sufficiently large for $D$ to be less than one. Conversely, the wave is fully dispersed wherever $D > 1$.

The interesting fact has thus emerged that in the near-equilibrium limit the shock waves can be partly dispersed when $\delta$ is sufficiently small, and the concept of an

equivalent bulk viscosity can be spurious. Moreover, this critical size of $\delta$ depends on the geometry, being $O(\epsilon)$ and $O(\epsilon^4)$ for planar and axisymmetric configurations respectively.

Whilst $D$ can be determined formally for any particular body shape, we can provide an estimate of the position, on the front shock of all bodies, at which $D = 1$. If we assume that this position is sufficiently far from the body for the $r^{-\frac{3}{4}}$ decay (Whitham 1952) to hold in the vicinity of this position then we may estimate the value of $R$ at the critical point by

$$R_c^{\frac{3}{4}} \simeq \frac{M_{f0}^2 \epsilon^4}{\delta} \left( \frac{\Gamma_{f0} \mathscr{W}_0}{2^{\frac{1}{2}} \beta_{f0}^2} \right)^{\frac{1}{2}}, \tag{5.28}$$

where

$$\mathscr{W}_0 = \int_0^{\alpha_0} \mathscr{W}(y)\, dy \tag{5.29}$$

and $\alpha_0$ is the first zero of $\mathscr{W}$ in $\alpha > 0$. Normally $\mathscr{W}_0$ is rather insensitive to the body shape, and for the purpose of illustration we assume a value which actually holds for a semi-infinite body with a parabolic nose, namely $\mathscr{W}_0 \simeq 0{\cdot}2$. $R_c$ is quite sensitive to the Mach number, and if we choose $M_{f0} = 2{\cdot}0$, we find that $D = 1$ when $r$ is approximately $0{\cdot}5\epsilon^{-4}$ body lengths; at larger radii the shock is fully dispersed, and despite the fact that ord $\delta = \epsilon^4$ the bulk viscosity (which can *only* be used where $D \gg 1$) may still be comparatively large, as discussed in § 4.4.

### 5.3. *The case* ord $\lambda > 1$

In the near-frozen limit $\lambda \to \infty$ we may iterate on (5.6):

$$\partial(\mathscr{L}_f U^{(1)})/\partial\xi + \lambda^{-1} \beta_{f0} A U_\xi^{(1)} = O(\lambda^{-2}). \tag{5.30}$$

A single integration leads exactly to (4.20), and the results of § 4.2 apply directly.

### 5.4. *Numerical solutions*

In view of the complexity of the problem when there are no small (or large) parameters, numerical calculations have been carried out for a particular body shape. The shape which was chosen was a semi-infinite cylinder with a parabolic nose; referring to (2.9),

$$f(x) = \begin{cases} x - \frac{1}{2}x^2, & 0 \leqslant x \leqslant 1, \\ \frac{1}{2}, & 1 < x. \end{cases}$$

Figure 1 presents $\mathscr{W}$ for this particular body.

The matter of multi-valuedness is obviously dealt with most easily with a knowledge of the shape of the characteristics, and it was felt (with justification, we feel in hindsight) that the shock fitting would be best implemented via a direct solution of (5.11) with (5.10) providing values for the primitive variables (e.g. pressure). In fact, the numerical calculations were performed not on (5.11), but on the following equivalent equation:

$$2\lambda R Z_{\alpha RR} + (2R Z_{RR} + Z_R)[Z_\alpha + 1 - k\mathscr{W}'(\alpha) R^{\frac{1}{2}}] + (A\beta_{f0} R + \lambda) Z_{\alpha R} = \tfrac{1}{2} k \mathscr{W}'(\alpha) R^{\frac{1}{2}}, \tag{5.31}$$

where

$$\xi = Z + \alpha - k\mathscr{W}(\alpha) R^{\frac{1}{2}}, \tag{5.32}$$

$$k = M_{f0} K_f (2\beta_{f0})^{-\frac{1}{2}}, \tag{5.33}$$

$$\tfrac{1}{2} K_f U^{(1)} = (\partial\xi/\partial R)_\alpha. \tag{5.34}$$

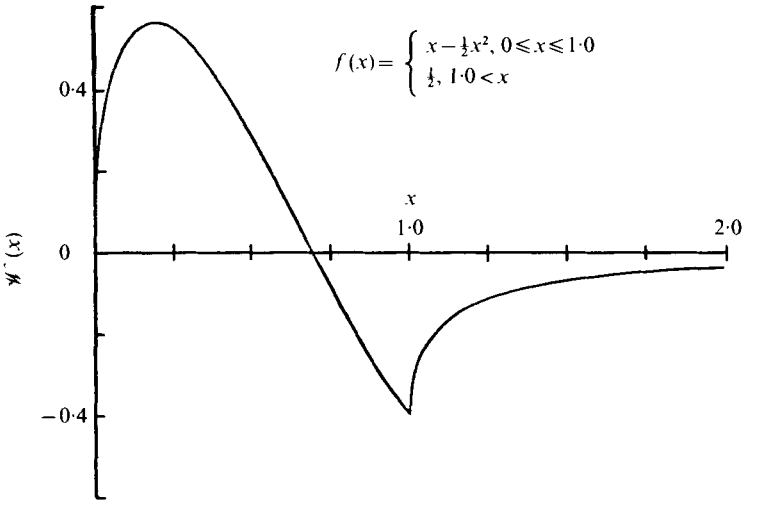


FIGURE 1. $\mathscr{W}(x)$ for a semi-infinite cylinder with a parabolic nose.

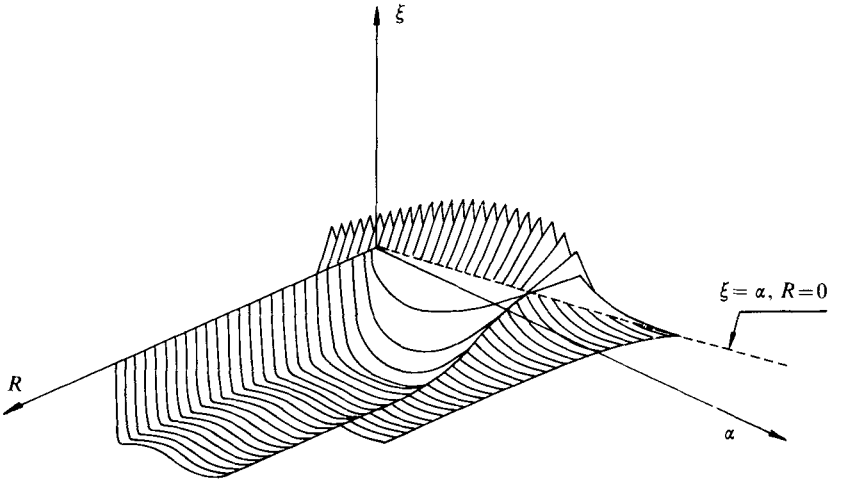


FIGURE 2. Numerical solutions of the small-$\delta$, parabolic-nose problem: a typical view of $\xi(\alpha, R)$ from the octant $\alpha < 0$, $R < 0$, $\xi < 0$ (the surface is viewed from underneath, approximately in the direction of the arrow marked $a$ in figure 3).

Equation (5.31) is derived by transforming (5.6) with the aid of (5.34) in a manner exactly equivalent to the derivation of (5.11) from (5.9). Equation (5.31) was solved instead of (5.11) simply because (5.11) was found after the computations had been completed. Despite the simpler structure of (5.11) we are in no doubt that differences between numerical solutions of (5.11) and (5.31) would be utterly negligible (except, possibly, at large $\alpha$ and $R$) for the following reason: our explicit finite-difference scheme, which uses a six-star molecule, employs (5.31) to express the value of $\xi$ at one point in the $\alpha$, $R$ plane in terms of the values of $\xi$ at the other five points. Hence the only difference between the algorithms from the two equations would be this final expression for $\xi$ at the sixth point; numerical answers would therefore be virtually

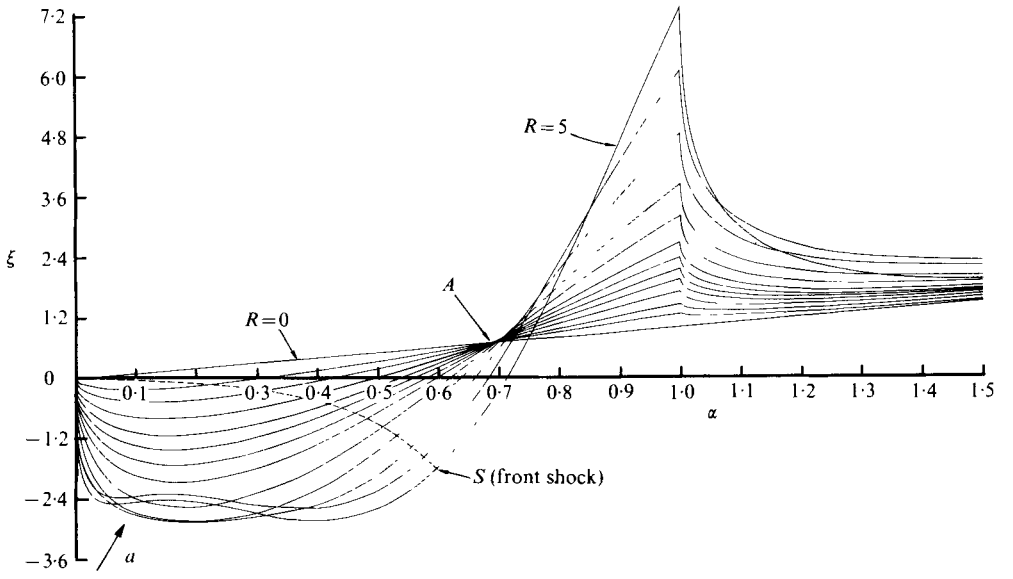


FIGURE 3. A numerical solution of the small-$\delta$ equation for the parabolic nose, depicting $\xi$ *vs.* $\alpha$ for fixed $R$. The finite-difference grid in the $\alpha$, $R$ plane has an expanding step size and successive curves in this figure do not correspond to identical changes in $R$. The relevant parameters are $\hat{\delta} = \epsilon^4$, $\lambda = 1{\cdot}0$, $M_{f0} = 2{\cdot}0$, $\Gamma_{f0} = 1{\cdot}2$.

identical (the computations were carried out in double precision anyway), except perhaps for a build-up of cumulative errors at large values of $\alpha$ and $R$. Note that the present analogue of (5.11) is

$$2YX_{\alpha YY} + X_\alpha(2YX_{YY} + X_Y) + (2Y+1)X_{\alpha Y} = 0.$$

Be that as it may, (5.32) constitutes a 'subtraction of the singularity' (Ames 1965, p. 411) and it leads to homogeneous boundary conditions on $Z$:

$$Z(0,R) = 0 = Z(\alpha,0), \quad Z_R(\alpha,0) = 0. \tag{5.35}$$

Subject to these conditions, (5.31) was solved numerically using first-order explicit finite differences, to obtain the values of $\xi$ in the quadrant $\alpha > 0$, $R > 0$. The solution surface is rather complicated in shape, and for this reason we include figure 2, in which the surface is viewed from the octant $\alpha < 0$, $R < 0$, $\xi < 0$.

Unfortunately, the computational algorithm possesses an instability which manifests itself when $\lambda$ is approximately less than 0·3, but we can turn to § 5.2 for analytical solutions when $\lambda$ is small.

Figure 3 exhibits solution curves $\xi$ *vs.* $\alpha$ ($0 \leqslant \alpha \leqslant 1{\cdot}5$) for fixed $R$ in the range 0–5·0. There are several striking features of the curves, but it should be pointed out first that in *frozen* flow the values of $\xi$ increase *monotonically* with $R$ for fixed $\alpha$; in fact, $\xi$ is then proportional to $R^{\frac{1}{2}}$ (Whitham 1952). Moreover, in frozen flow $\xi = \alpha$ at any value of $\alpha$ which is a zero of $\mathscr{W}(\alpha)$, so that in such circumstances each and every curve, regardless of the value of $R$, would pass through the point marked $A$ in figure 3.

It is apparent at a glance that the behaviour is *not* monotonic with respect to $R$, and as $R$ increases the curves *do not* all pass through the point $A$. The evolution of the kink near the front is illustrated clearly in figure 2. We have convincing explanations for these phenomena, but we shall postpone further discussion of the kink until we deal

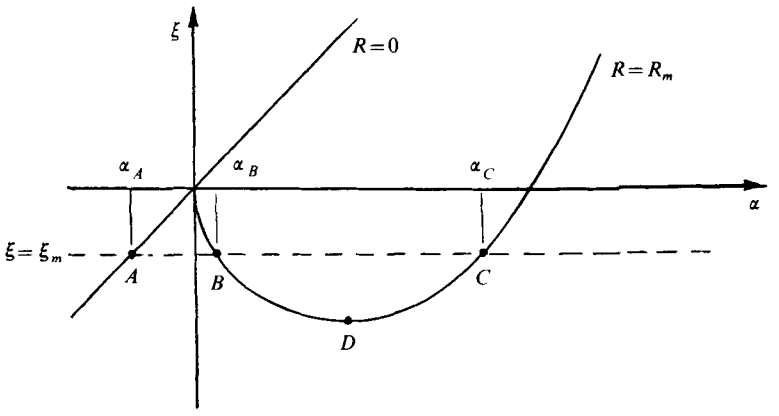


FIGURE 4. A typical solution curve near the wave front; small $R$.

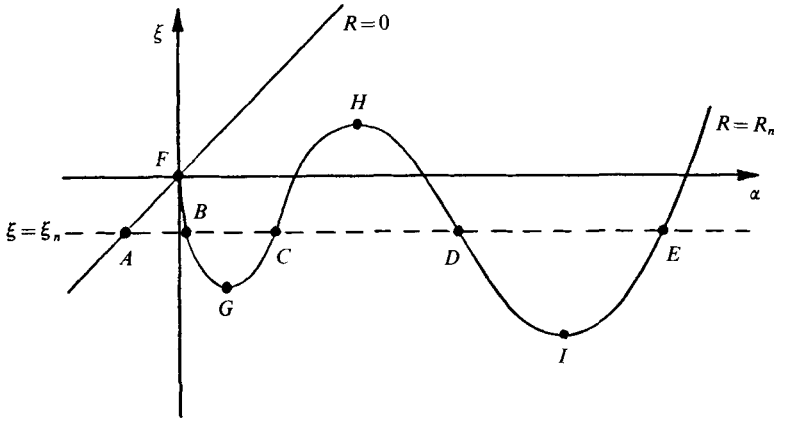


FIGURE 5. A typical solution curve near the wave front; larger $R$.

with the shock fitting. Meanwhile, we observe [see (5.34)] that perturbations vanish wherever $(\partial\xi/\partial R)_\alpha = 0$. For the present body $\mathscr{W}$ possesses a zero at $\alpha \simeq 0{\cdot}69$, and in frozen flow the characteristic $\alpha = 0{\cdot}69$ would be a straight line $\xi =$ constant which would reach infinity and which would constitute the 'centre' of the wave along which the pressure is just the ambient pressure. Evidently, in the presence of the non-equilibrium effects the characteristic $\alpha = 0{\cdot}69$ is no longer straight, and in fact figure 3 shows that the centre of the wave tilts backwards (i.e. in the direction of increasing $\xi$) towards the equilibrium direction as $R$ increases.

Turning now to the front region, figures 4 and 5 present typical shapes of the solution as $\xi$ *vs.* $\alpha$ for small $R$ (where conditions are frozen) and larger $R$ (where a lack of equilibrium prevails). In figure 4 it is seen that in a certain range of $\xi$ the solution is triple-valued (this is a familiar phenomenon in gasdynamics). In figure 5 the situation is more complicated, in so far as *five* characteristics (corresponding to the points marked $A$, $B$, $C$, $D$ and $E$) pass through the point in physical space given by $\xi_n$, $R_n$. The envelopes of the characteristics, defined by $(\partial\xi/\partial\alpha)_R = 0$, are correspondingly complex, being four in number (as opposed to two in frozen flow) and corresponding to the points marked $F$, $G$, $H$ and $I$. The evolution of the envelopes in physical space is

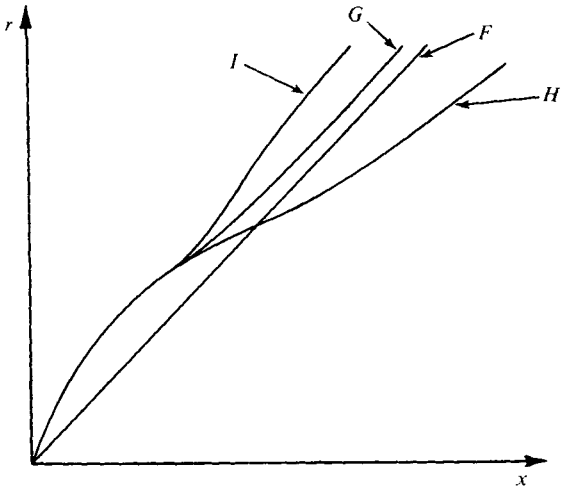


FIGURE 6. A sketch of a front envelope in a relaxing gas.

illustrated in figure 6. The 'splitting' of the front frozen branch of the envelope into the branches marked $I$ and $H$ corresponds to a flattening of the curve in the vicinity of the point marked $D$ in figure 4.

The multi-valuedness obviously has to be rectified through the insertion of a shock (presently 'shock' will denote the *discontinuous* part of a wave); although an algorithm for fitting the rear shock has been formulated in principle, it has been found to be too expensive in computer time and it has therefore not been incorporated into the computer program. Whilst information about the complete wave profile is attractive, the present calculations (which are new in themselves) provide us with important quantitative details ahead of the centre of the wave (the centre being the position at which the perturbations vanish). In passing we note that in the present context the asymptotic wave profile is evidently *not* symmetrical about its centre, unlike frozen flow. The fitting technique, which uses an iterative interpolation, is based on the 'mean wavelet direction' property of weak waves (e.g. Liepmann & Roshko 1957, p. 93; Whitham 1952), which in our notation reads

$$2\frac{d\xi_s}{dR_s} \simeq \left(\frac{\partial \xi}{\partial R}\right)_{\alpha_1} + \left(\frac{\partial \xi}{\partial R}\right)_{\alpha_s}. \tag{5.36}$$

Having determined the shock path up to a certain value of $R$, a sensible guess is made at the shock position at a larger $R$, and numerical interpolation is used to express the right-hand side of (5.36) as a polynomial in $R$. An integration of (5.36) then yields an improved estimate of the shock position, and the process is repeated until an error criterion is satisfied. The shock is started off by fitting a frozen shock (Whitham 1952) over the first step.

It is obvious, on physical grounds, that the 'outermost' solutions must be chosen during the fitting, so that if the dotted line represents the determined shock position at the particular $R$ in figures 4 and 5, the discontinuous jumps are represented by $AC$ and $AE$ in the two figures.

It is important to note that each characteristic is cut off when it meets the shock, and it will *not* appear at larger values of $R$. Consequently, the characteristics associated

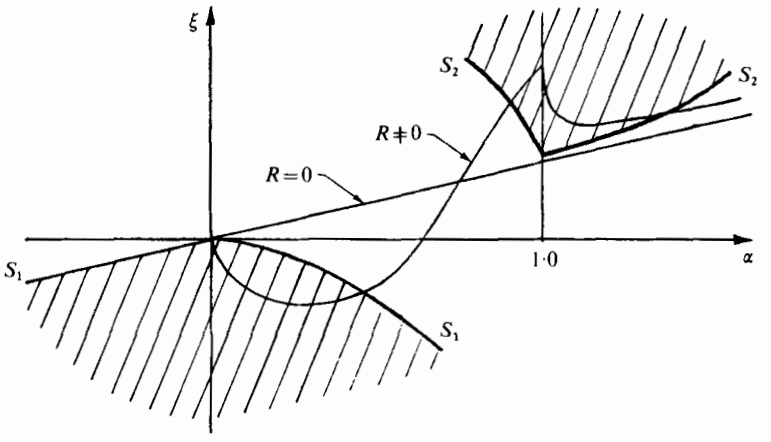


FIGURE 7. Typical front- and rear-shock loci in the computational plane, illustrating the discarded solutions. $S_1$, front shock; $S_2$, rear shock; ////, discarded solutions.

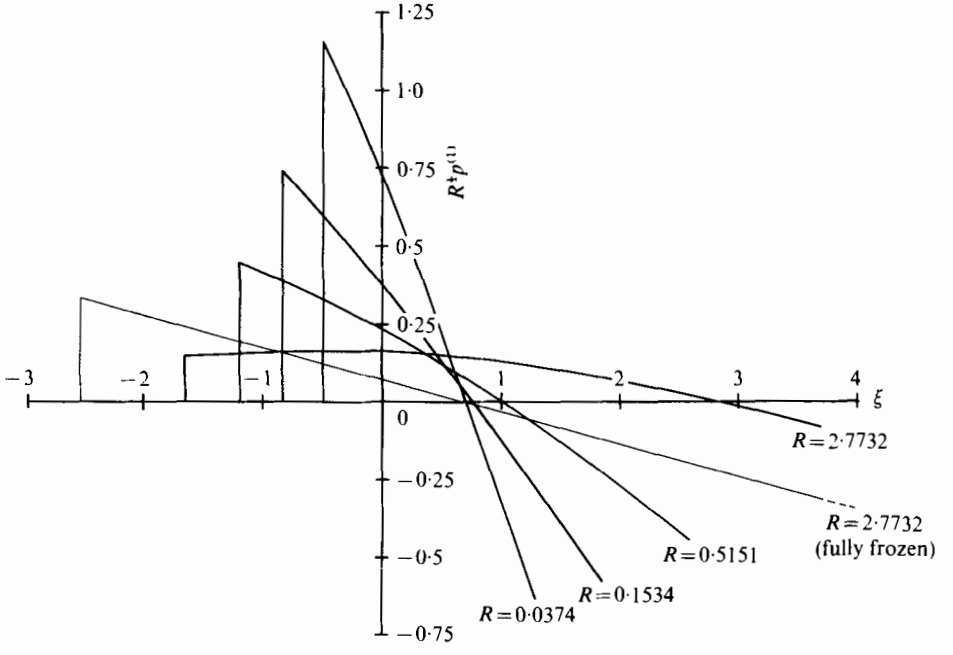


FIGURE 8. The pressure profiles across the wave, excluding the rear shock. Parameters as for figure 30.

with the kinks are truncated relatively close to the body, and the complicated envelope disappears as the shock is fitted, as it should; these points are illustrated in figure 7.

Figure 8 presents the pressure distributions across the wave (excluding the tail); attenuation distorts the profiles away from the customary $N$-shape. Finally, figures 9 and 10 provide the shock loci and strengths for various values of the parameters, and they illustrate the overall dissipative influences of the non-equilibrium phenomenon.

In view of all these ramifications, it now becomes clear why a kink develops near the front. We know from (5.34) that, as the perturbations decrease, the spacing between

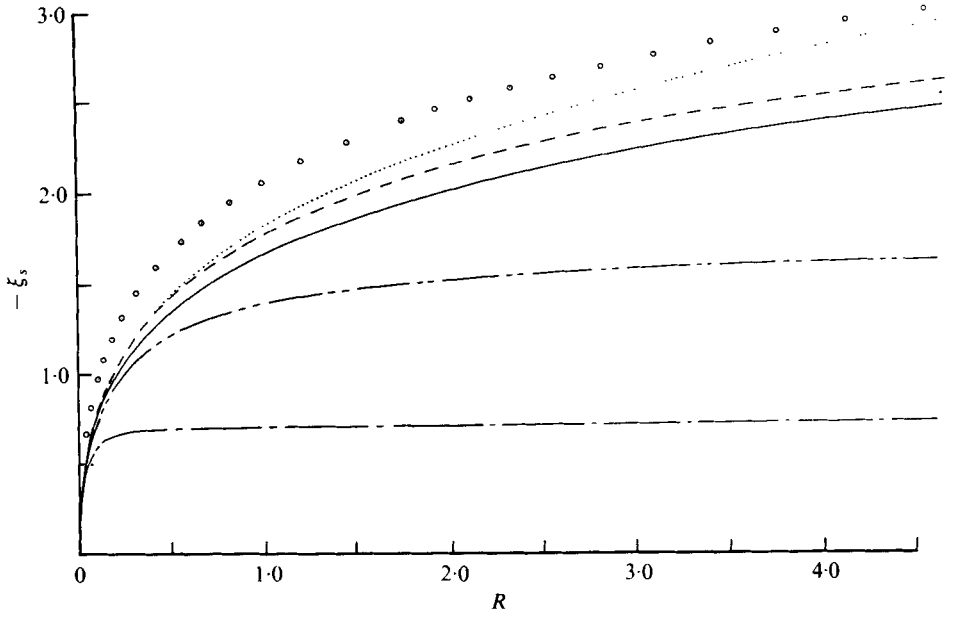


FIGURE 9. Front-shock co-ordinates for different values of $\hat{\delta}/\epsilon^4$ and $\lambda$. The graph includes a comparison, for $\lambda = 10$, between the numerical results and the prediction of (4.28) and (4.29). ·····, fully frozen (Whitham); – – –, approximate analytical, $\lambda = 10{\cdot}0$, $A = 1{\cdot}0$. Numerical: ⊙, singularity not removed; ——, $\lambda = 10{\cdot}0$, $\hat{A} = 1{\cdot}0$; —··—, $\lambda = 1{\cdot}0$, $\hat{A} = 1{\cdot}0$; —·—, $\lambda = 1{\cdot}0$, $\hat{A} = 10{\cdot}0$.

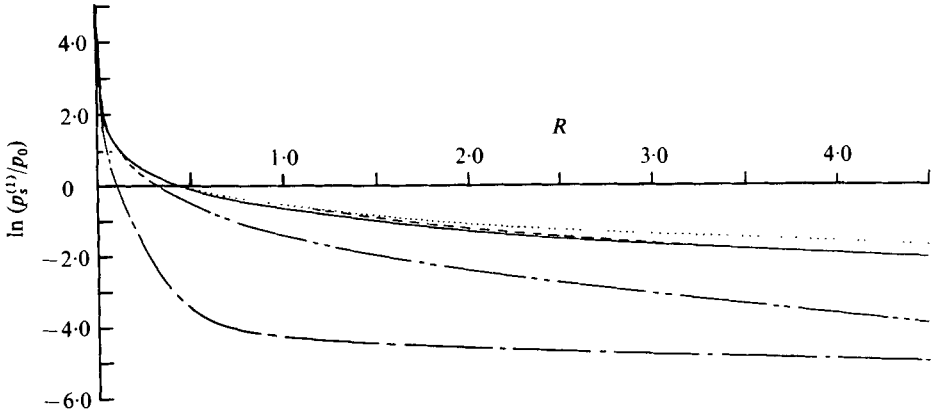


FIGURE 10. Front-shock strengths for different values of $\hat{\delta}/\epsilon^4$ and $\lambda$. Curves as in figure 9.

successive curves on the $\xi$ *vs.* $\alpha$ graph decreases as well. Consequently, the only way in which the strength of the discontinuity can be made to diminish over and above the usual geometric factor is through the appearance of the kinks; these lead to a reduction in the spacing between successive curves in the region in figure 3 through which the shock passes. It should be reiterated that the curves in figure 3 do not correspond to equal intervals in $R$, because the grid is an *expanding* one.

Another interesting point is that, since $\Delta(Y) > 0$, the non-monotonicity in $\xi$ with respect to $R$ is hinted at by (5.18).

## 6. Very small $\delta$

Despite the fact that under normal aeronautical circumstances $\epsilon$ is very small (0·05 typically), we include a discussion of the situation ord $\delta < \epsilon^4$ for the sake of completeness. This section encompasses the flow about bodies which are 'not so slender', such as bullets.

Turning to (5.6), it is apparent that when $A$ is small we can simply obtain a regular perturbation solution. Let us first rewrite (5.6) as follows:

$$(\lambda\,\partial/\partial\xi + 1)\,(w_R + \tfrac{1}{2}K_f R^{-\frac{1}{2}} w w_\xi) + \mathscr{A} w_\xi = 0, \tag{6.1}$$

where
$$w = R^{\frac{1}{2}} U^{(1)}, \quad \mathscr{A} = \tfrac{1}{2}\beta_{f0} A. \tag{6.2}$$

If we seek a solution [subject to (4.24)] of the form

$$w = w^{(0)} + \mathscr{A} w^{(1)} + \ldots, \tag{6.3}$$

we find that $w^{(0)}$ is of course the classical frozen solution [$k$ is defined in (5.33)]

$$w^{(0)} = -M_{f0}(2\beta_{f0})^{-\frac{1}{2}} \mathscr{W}(\alpha), \quad \xi(\alpha, R) = \alpha - k\mathscr{W}(\alpha) R^{\frac{1}{2}} \tag{6.4}$$

and that $w^{(1)}$ is governed by

$$(\lambda\,\partial/\partial\xi + 1)\{w_R^{(1)} + \tfrac{1}{2}K_f R^{-\frac{1}{2}}[w^{(0)} w_\xi^{(1)} + w_\xi^{(0)} w^{(1)}]\} + \omega_\xi^{(0)} = 0. \tag{6.5}$$

Transforming the independent variables from $\xi$ and $R$ to $\alpha$ and $R$ with the aid of (6.4) gives

$$(\partial/\partial\alpha + T/\lambda)\,[w_R^{(1)} + \tfrac{1}{2}K_f R^{-\frac{1}{2}} T w_\alpha^{(0)} w^{(1)}] = -\lambda^{-1} w_\alpha^{(0)}, \tag{6.6}$$

where
$$T(\alpha, R) = 1 - k\mathscr{W}'(\alpha) R^{\frac{1}{2}} \equiv (\partial\xi/\partial\alpha)_R. \tag{6.7}$$

After two integrations of (6.6) it transpires that

$$w^{(1)}(\alpha, R) = \lambda^{-1} T^{-1} \int_0^R T(\alpha, y)\,\Omega(\alpha, y) \exp\,[-\lambda^{-1}\xi(\alpha, y)]\,dy, \tag{6.8}$$

where
$$\Omega(\alpha, R) = \frac{M_{f0}}{(2\beta_{f0})^{\frac{1}{2}}} \int_0^\alpha \mathscr{W}'(y) \exp\,[\lambda^{-1}\xi(y, R)]\,dy. \tag{6.9}$$

In accordance with our previous considerations, we declare that the non-equilibrium effects are relegated to second-order terms when ord $A \leqslant \epsilon^4$, i.e. when ord $\delta \leqslant \epsilon^8$.

## 7. Conclusions

This paper describes the far-field wave behaviour for complete spectra of $\epsilon$, $\delta$ and $\lambda$ by distinguishing four separate levels of $\delta$ and thereafter allowing ord $\lambda$ to be less than one, equal to one or greater than one.

When $1 \geqslant$ ord $\delta > \epsilon^4$, the wave head emanating from the tip is a frozen Rankine–Hugoniot shock wherever $r \lesssim \lambda/\delta$. If ord $(\lambda\epsilon^4/\delta) < 1$, which is true in most aeronautical circumstances, the behaviour of this shock, given by (4.9), is independent of the overall shape of the body, being related solely to the tip angle. When ord $(\lambda\epsilon^4/\delta) \geqslant 1$ a near-frozen field, including the rear shock, is described by (4.22), (4.28) and (4.29); again, frozen shocks extend as far as $r \lesssim \lambda/\delta$. Sufficiently far from the body the shock waves will inevitably be fully dispersed. In fact, if the body is finite, linear

theory holds when ord $(\lambda\delta) > \epsilon^4$; if ord $(\lambda\delta) < \epsilon^4$ we find that the shocks are structured by an equivalent bulk viscosity [see (4.75)] which may overwhelm the shear viscosity when the humidity is low. Clearly, the importance of the influence of the non-equilibrium process (as opposed to transport phenomena) on the shock waves' structure can be assessed simply by comparing the relevant diffusivities.

When ord $\delta = \epsilon^4$ the behaviour of the frozen bow shock is more complex, but it is described by (4.9) when $r \ll \lambda\epsilon^{-4}$; details of the initial departure from this law may be found in I. Perturbation solutions have been obtained for small and large $\lambda$: when ord $\lambda < 1$ it transpires that an equivalent bulk viscosity may not be used in certain domains, and for a given body one can determine the critical distance at which the wave structures change from the partly to the fully dispersed type. A universal approximation (5.28) insensitive to the overall shape of most aircraft but quite sensitive to the Mach number is also supplied for this position on the *bow* shock. If the body shape is such that a shock wave forms away from the body, the wave can evolve through stages of full, partial and then full dispersal. Even when ord $\delta = \epsilon^4$, the equivalent bulk viscosity, where it is valid, can be larger than the shear viscosity. When ord $\lambda > 1$, we recover the near-frozen solution of § 4.2. Numerical solutions have also been found, in order to cope with the situation $\lambda = \text{ord}\, 1 = \delta/\epsilon^4$. These calculations were performed for a semi-infinite cylinder with a parabolic nose, and the bow shock has been fitted. When $\lambda$ is large, the computations compare favourably with the near-frozen perturbation solution.

When $\epsilon^8 < \text{ord}\, \delta < \epsilon^4$, a perturbation solution is available; it allows us to find the small correction to a fully frozen flow. This result could be applicable to bodies which are not so slender, such as bullets.

When ord $\delta \leqslant \epsilon^8$, the first-order solution is unequivocally the one from classical frozen theory.

Some of the material in this (as well as the companion) paper was presented at the Seventh International Symposium on Nonlinear Acoustics, Virginia Polytechnic Institute and State University, Blacksburg, Virginia, U.S.A., 19–21 August 1976.

## REFERENCES

AMES, W. F. 1965 *Nonlinear Partial Differential Equations in Engineering*, vol. 1. Academic Press.

BLYTHE, P. A. 1969 *J. Fluid Mech.* **37**, 31.

CHONG, T. H. & SIROVICH, L. 1970 *Phys. Fluids* **13**, 1990.

CHONG, T. H. & SIROVICH, L. 1973 *J. Fluid Mech.* **58**, 53.

CHOU, D. C. 1972 *Astron. Acta* **17**, 625.

CHOU, D. C. & CHU, B.-T. 1971 *J. Fluid Mech.* **50**, 355.

CLARKE, J. F. 1961 *J. Fluid Mech.* **11**, 577.

CLARKE, J. F. 1965 *Cranfield Inst. Tech. Aero. Rep.* CoA 182.

CLARKE, J. F. & MCCHESNEY, M. 1976 *The Dynamics of Relaxing Gases*. Butterworths.

CLARKE, J. F. & SINAI, Y. L. 1977 *J. Fluid Mech.* **79**, 499.

COLE, J. D. 1968 *Perturbation Methods in Applied Mathematics*. Blaisdell.

HAYES, W. D. & PROBSTEIN, R. F. 1966 *Hypersonic Flow Theory. Part* I. Academic Press.

HODGSON, J. P. 1973 *J. Fluid Mech.* **58**, 187.

HODGSON, J. P. & JOHANNESEN, N. H. 1971 *J. Fluid Mech.* **50**, 17.

JONES, J. G. 1964 *J. Fluid Mech.* **19**, 81.

KRAIKO, A. N. 1966 *Prikl. Mat. Mekh.* **30**, 793.

LANDAHL, M. & LOFGREN, P. 1973 *N.A.S.A. Contractor Rep.* CR-2339.

LEIBOVICH, S. & SEEBASS, A. R. 1974 *Nonlinear Waves.* Cornell University Press.

LI, T. Y. & WANG, K. C. 1962 *Rensselaer Polytech. Inst. Aero. Engng Dept. Tech. Rep.* TR-6201.

LICK, W. 1967 *Adv. Appl. Mech.* **10**, 1.

LIEPMANN, H. W. & ROSHKO, A. 1957 *Elements of Gasdynamics.* Wiley.

LIGHTHILL, M. J. 1956 *Surveys in Mechanics* (ed. G. K. Batchelor & R. M. Davies). Cambridge University Press.

LILLEY, G. M. 1965 The structure of shock waves at large distances from bodies travelling at high speeds. *Proc. 5th Cong. Int. d'Acoustique Liege* (ed. D. E. Commings), vol. 2, pp. 109–162.

MURRAY, J. D. 1968 *J. Math. & Phys.* **47**, 111.

OCKENDON, H. & SPENCE, D. A. 1969 *J. Fluid Mech.* **39**, 329.

PARKER, D. F. 1975 Contribution to *17th Brit. Theor. Mech. Coll.*

PIERCE, A. D. & MAGLIERI, D. J. 1972 *J. Acoust. Soc. Am.* **51**, 702.

RUDENKO, O. V., SOLUYAN, S. I. & KHOKHLOV, R. V. 1974 Problems of the theory of nonlinear acoustics. *Proc.* 1973 *Symp. Finite-Amplitude Wave Effects in Fluids* (ed. L. Bjørnø), IPC Science & Tech., or Soviet Physics-Acoustics, **20**, 271.

RYZHOV, O. S. 1971 *Prikl. Mat. Mekh.* **35**, 972.

SANCHEZ-PALENCIA-HUBERT, J. 1976 *Int. J. Engng Sci.* **14**, 567.

SEDNEY, R. & GERBER, N. 1963 *A.I.A.A. J.* **1**, 2482.

SINAI, Y. L. 1975 Ph.D. thesis, Cranfield Institute of Technology.

SINAI, Y. L. 1976 *Phys. Fluids* **19**, 1059.

SIROVICH, L. 1968 *Phys. Fluids* **11**, 1424.

STEPHENSON, J. D. 1960 *N.A.S.A. Tech. Note* D-327.

SUTHERLAND, L. C. 1975 Review of experimental data in support of a proposed new method for computing atmospheric absorption losses. *Wyle Lab. Transportation* DOT-TST-75-87.

TKALENKO, R. A. 1975 *Prikl. Mat. Mekh.* **39**, 647.

VAN DYKE, M. 1975 *Perturbation Methods in Fluid Mechanics*, annotated edition. Parabolic Press.

VARLEY, E. & ROGERS, T. G. 1967 *Proc. Roy. Soc.* A **296**, 498.

WEGENER, P. P., CHU, B-T. & KLIKOFF, W. A. 1965 *J. Fluid Mech.* **23**, 787.

WHITHAM, G. B. 1952 *Comm. Pure Appl. Math.* **5**, 301.

WHITHAM, G. B. 1974 *Linear and Nonlinear Waves.* Wiley.